Fluorescent Probes

DOI: 10.1002/ange.200900369

Fluorescence Detection of Single-Nucleotide Polymorphisms with a Single, Self-Complementary, Triple-Stem DNA Probe**

*Yi Xiao, Kory J. I. Plakos, Xinhui Lou, Ryan J. White, Jiangrong Qian, Kevin W. Plaxco, and H. Tom Soh**

Single-nucleotide polymorphisms (SNPs) can serve as an important indicator of genetic predisposition towards disease states or drug responses.[1,2a] The detection of rare base substitutions within populations of DNA molecules is essential for studying the effects of DNA damage and for pool screening for SNPs.[2b] There is thus an urgent need for technologies suitable for sensitive, high-throughput SNP detection.[3] Ideally, these methods would be single-step, reagentless, room-temperature assays, suitable for clinical and research use and compatible with microarray technologies for massive analysis.[4]

Unfortunately, current technologies satisfy only some of these requirements. For example, enzymatic SNP-detection methods, such as endonuclease digestion,[5,6] primer extension,[7] and ligation assays,[8] are very sensitive and specific even at room temperature, but are complex, multistep techniques that often require separation of the resultant products before the presence of the target sequence can be determined. These limitations have motivated the development of simpler fluorescence-based assays with molecular beacons,[9–11] binary probes,[12,13] forced intercalation of thiazole orange (FIT) probes,[14] and base-discriminating fluorescent (BDF) probes.[15]

Molecular beacons (MBs) are stem-loop oligonucleotides with self-complementary 5′ and 3′ ends that bring a fluorophore–quencher pair into close proximity in the absence of a target. Hybridization to a complementary target disrupts the stem-loop and thereby induces a large increase in fluorescence upon segregation of the pair.[16] MBs are well-suited for rapid SNP detection as they enable reagentless and quantitative analysis without the need for separation steps.[9–10,16–19] However, their reliance on the melting temperature of probe–target duplexes as the basis for mismatch discrimination limits potential targets to those whose melting temperatures can be distinguished through precise temperature control. With a few exceptions,[20,21] MBs typically do not perform well at room temperature without significant, empirical optimization of their thermodynamics.[22]

Binary-probe assays avoid these limitations and enable SNP analysis at room temperature.[8,12,13,23–25] These assays are based on the use of a pair of nonidentical DNA probes that form relatively short (7- to 10-nucleotide) duplexes at sites adjacent to a target sequence. Signal detection is possible through a ligation reaction,[8] fluorescence,[23] or colorimetric[24] readouts, or by resonance energy transfer.[25] These short hybrids are very sensitive to mismatches and can readily distinguish single nucleotide substitutions. Therefore, the approach is specific, sensitive, and reliable. However, the addition of multiple exogenous reagents is required. Other alternatives include thiazole orange modified FIT probes[14] and BDF probes,[15] which are modified single-stranded DNA molecules that produce only weak fluorescence in the absence of a target, but emit strong fluorescence upon target recognition. However, the specificity of these probes for SNP detection is highly dependent on the length of the linker, the conjugation site, and the sequence of the mismatched base pairs. Thus, there remains a need for simple and efficient room-temperature SNP assays without significant probe optimization.

We present herein a strategy that combines advantages of MBs and binary probes in a single triple-stem DNA structure for robust single-step SNP detection in a homogeneous, room-temperature system without addition of exogenous reagents. This probe produces a negligible signal in the presence of single-base-mismatched targets, but hybridization to a perfectly matched target induces a significant conformational change that results in a large increase in the fluorescence signal (Figure 1). Importantly, the triple-stem probe architecture enables tuning of its sensitivity and selectivity towards specific target sequences over a wide temperature range.

The triple-stem DNA-based SNP sensor consists of a single 68-base DNA strand, **1**, that has been modified with a CAL Fluor Red 610 (FR610) fluorophore at the 3′ terminus and a Black Hole Quencher (BHQ) at an internal position. At room temperature, the probe self-hybridizes into three separate, seven-base-pair (bp) Watson–Crick stems that form a discontinuous, 21 base double helix[26] (Figure 1a, left). In the absence of a target, this relatively rigid triple-stem structure holds the fluorophore in close proximity to the quencher; this arrangement results in very limited fluorescence (Figure 1b). Upon hybridizing to a perfectly matched 17 nucleotide target (PM; **2**), the triple-stem structure is

[*] Dr. Y. Xiao, K. J. I. Plakos, Dr. X. H. Lou, Dr. J. R. Qian, Prof. H. T. Soh
Materials Department, Department of Mechanical Engineering
University of California, Santa Barbara
Santa Barbara, CA 93106 (USA)
Fax: (+1) 805-893-8651
E-mail: tsoh@engr.ucsb.edu
Dr. R. J. White, Prof. K. W. Plaxco
Department of Chemistry, University of California, Santa Barbara
Santa Barbara, CA 93106 (USA)

[**] This research was supported by the Office of Naval Research (N00014-08-1-0469), by the National Institutes of Health (R21 EB008215), and by the Institute for Collaborative Biotechnologies through grant DAAD19-03-D-0004 from the U.S. Army Research Office.

Supporting information for this article is available on the WWW under http://dx.doi.org/10.1002/anie.200900369.

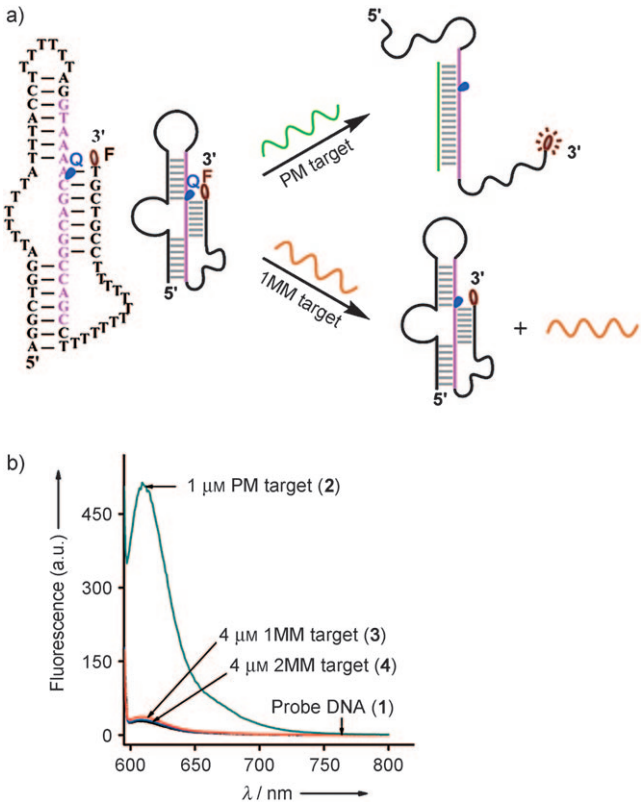

Figure 1. a) Mechanism of the SNP sensor. In the presence of a perfectly matched (PM) target, the folded triple-stem DNA structure is disrupted and fluoresces. In contrast, single-base-mismatched (1MM) or two-base-mismatched (2MM) targets do not destabilize the discontinuous duplex, and the probe maintains its triple-stem structure with quenched fluorescence. b) Emission spectra of the triple-stem probe **1** (0.5 μM) following incubation at room temperature with the PM target **2**, the 1MM target **3**, the 2MM target **4**, or no target. The fluorescence signal was measured at $\lambda_{ex} = 590$ nm and $\lambda_{em} = 610$ nm, and all targets were 17 bases in length.

disrupted, with separation of the fluorophore–quencher pair (Figure 1a) and induction of a 29-fold increase in emission intensity (Figure 1b). In contrast, when the probe was challenged with a target containing a single base mismatch in the middle of the sequence (1MM; **3**), we observed only a 1.3-fold increase in emission intensity, even at a fourfold higher concentration (Figure 1b); a two-base-mismatched target (2MM; **4**) did not produce any detectable increase in fluorescence (Figure 1b). An important feature of our probe structure is that its design requires minimal optimization. As an example, we synthesized a second triple-stem probe, **5**, with an A-to-G substitution at position 39 (from the 5′ end). The sequence of this probe matches that of the 1MM target **3** perfectly, and the probe is thus mismatched with the PM target **2**. As expected, we observed a large (26-fold) increase in emission intensity upon addition of the 1MM target **3**, and minimal signal enhancement was observed with the PM target **2** (see Figure S1 in the Supporting Information).

The thermodynamic stability of both the probe itself and the probe–target duplexes enables remarkable specificity for SNPs over a wide temperature range up to 60 °C. The triple-stem probe is assumed to exist in three different phases in the presence of targets:[27] phase 1, as a target–probe duplex; phase 2, as a folded probe; and phase 3, as a random coil (Figure 2a). At low temperatures, the probe hybridizes with

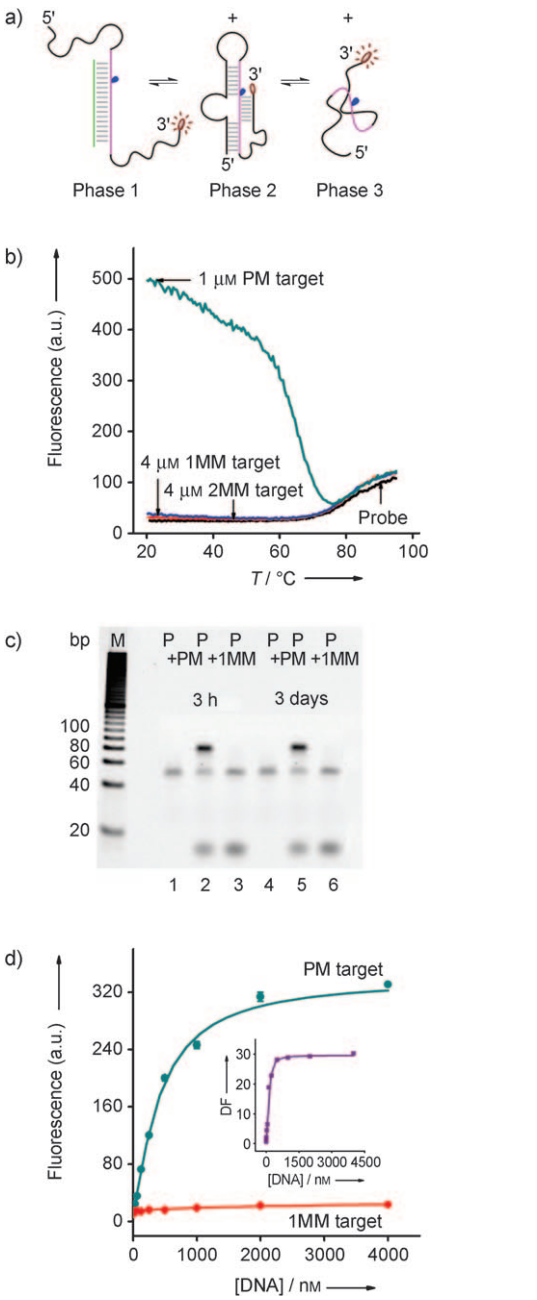

Figure 2. The triple-stem probe **1** displays excellent discrimination against mismatches. a) Proposed phase transitions of the triple-stem probe in the presence of targets at different temperatures. b) The SNP sensor retains its discrimination functionality up to 60 °C. Thermal denaturation curves of the probe only, and the probe hybridized with the PM target **2**, the 1MM target **3**, or the 2MM target **4**. c) Gel image of the triple-stem probe only (lanes 1 and 4), PM target **2**–probe samples (lanes 2 and 5), and 1MM target **3**–probe samples (lanes 3 and 6). One set of samples was equilibrated for 3 h (lanes 1–3), the other was equilibrated for three days (lanes 4–6). d) A calibration curve of the PM target **2** and the 1MM target **3** for the triple-stem probe. The inset shows the concentration dependence of the discrimination factor of 17 base targets in the presence of the probe (0.5 μM).

the PM target (phase 1), which gives rise to significantly increased fluorescence (Figure 2b). As the temperature increases, the duplex is destabilized, and the released probe apparently refolds into its native structure (phase 2), which results in significantly diminished fluorescence. For the PM target, the transition from the target–probe duplex to the self-complementary triple-stem structure occurred at 65 °C. At temperatures above 82 °C, the folded probe melted into random coils (phase 3), in which quenching efficiency is reduced, and a small increase in fluorescence was observed. In contrast, little fluorescence was observed for 1MM or 2MM targets at low temperatures (Figure 2b), and the signals in the presence of no target, the PM target, and mismatched targets merged at higher temperatures.

To investigate the kinetic response of the triple-stem probe, we performed time-resolved measurements with the PM target (1 μM) and mismatched targets (4 μM). We define the single-mismatch discrimination factor as the ratio of the net fluorescence intensity observed with the PM target to that observed with the 1MM target after subtraction of the background fluorescence; thus, a larger discrimination factor is indicative of greater specificity. Upon addition of the PM target to a solution of the native, quenched probe, we observed an exponential rise in fluorescence over time. In contrast, almost no signal change was observed with mismatched targets (see Figure S2 in the Supporting Information). The equilibration time constant for the PM target is approximately 78 min, which is similar to that observed for binary-probe methods[8,12] but slower than that of MBs.[9–10] The longer equilibration time presumably reflects the stability of the triple-stem structure ($T_m = 80.2$ °C).[28,29] However, this method compares favorably with enzyme-mediated SNP-detection methods:[5–8] A discrimination factor of 16 was obtained after 30 min, with signal saturation occurring at a discrimination factor of 28 after 3 h (see Figure S2 in the Supporting Information). Moreover, we did not observe any signal difference between samples that had been equilibrated for 3 h (Figure 2c, lanes 1–3) and samples that had been equilibrated for 3 days (Figure 2c, lanes 4–6). This result strongly suggests that we are operating in the equilibrium limit. Likewise, polyacrylamide gel electrophoresis indicated that equilibration was complete within 3 h and that only perfectly matched targets produced the 85 bp band corresponding to the probe–target duplex (Figure 2c, lanes 2 and 5). Under the conditions employed in this study, the calculated hybridization efficiency of our system is approximately 45 % (Figure 2c, lanes 1 and 2; lanes 4 and 5), which confirms that target concentration is an important factor for hybridization efficiency.

Titration experiments confirmed that the triple-stem probe displays remarkable specificity for perfectly matched targets, with minimal response to even substantially higher concentrations of mismatched targets. A peak discrimination factor of 30 was reached when the probe was titrated with the PM target (Figure 2d, inset); in contrast, we observed only a 1.5-fold increase in fluorescence intensity in the presence of the 1MM target at a concentration of 4 μM (see Figure S3 in the Supporting Information). We observed a high degree of discrimination over a wide target-concentration range up to 300 μM (data not shown); for example, a discrimination factor of 4 was found in a comparative analysis with 32 nM of each target, and a discrimination factor of 5 was found for 125 nM PM target versus 4 μM 1MM target (Figure 2d). The titration curve shows the nonlinear hyperbolic relationship between DNA-hybridization efficiency and target concentration;[30–32] it is reminiscent of an active-site titration in which the PM target has high affinity and the 1MM target has low affinity.

To confirm the general applicability of the triple-stem probe, we tested its capacity to discriminate against mismatched bases at different positions within the PM target. We found discrimination factors ranging from 5.6 to 28.4 (Table 1); the highest level of discrimination occurred with duplexes containing a C/C mismatch, whereas the lowest was observed with an A/A mismatch. This result is consistent with previous findings that the thermodynamics of mismatches depend on the identity of the mismatched base pair as well as the identity of its near neighbors.[33,34] The triple-stem probe also displayed excellent discrimination for shorter (15 base) and longer (19 base) targets (see Table S1 in the Supporting Information).

Table 1: Discrimination factors (DFs) of the triple-stem probe **1** for single-base-mismatched targets that differ from the 17 base PM target **2** (5′-GCTGGCCGTCGTTTTAC-3′; mismatches are marked in red).

DNA target sequence (5′–3′)	Peak gain	DF	Mismatched base pair
GCTGGCCGTCGTTTTAC	888.5		
GCTGGGCGTCGTTTTAC	113.4	7.8	G–G
GCTGGCGGTCGTTTTAC	80.9	10.9	G–G
GCTGGCCCTCGTTTTAC	31.3	28.4	C–C
GCTGGCCGACGTTTTAC	159.3	5.6	A–A
GCTGGCCGCCGTTTTAC	112.2	7.9	A–C
GCTGGCCGGCGTTTTAC	71.6	12.4	A–G
GCTGGCCGTGGTTTTAC	61.2	14.5	G–G
GCTGGCCGTAGTTTTAC	66.9	13.3	G–A
GCTGGCCGTCCTTTTAC	35.0	25.4	C–C
GCTGGCCGTCACTTTAC	55.9	15.8	C–A
GCTGGCCGTCGCTTTAC	65.9	13.5	A–C

We believe that the exceptional specificity of the triple-stem probe originates from its thermodynamic stability; at room temperature, the 21 bp discontinuous duplex in the probe is less stable than the continuous 17 bp PM target–probe duplex. Therefore, the presence of the PM target disrupts the native probe structure efficiently, which results in probe–target hybridization. In contrast, the native triple-stem structure is markedly more stable than duplexes containing a single mismatch and therefore inhibits 1MM target–probe hybridization.

To better understand the thermodynamic basis for this phenomenon, we used van 't Hoff plots[35] to investigate the enthalpy and entropy changes that describe the phase transition between phases 2 and 3 ($\Delta H^0_{2\to3}$ and $\Delta S^0_{2\to3}$), and found that the triple-stem probe undergoes large enthalpy and entropy changes ($\Delta H^0_{2\to3} = 30 \pm 3$ kcal mol^{-1}; $\Delta S^0_{2\to3} = 85 \pm 9$ cal mol^{-1} K^{-1}).

To construct the free-energy diagram[27,35] for the three phases of our probe, we measured the enthalpy and entropy

changes associated with the dissociation of duplexes with PM and 1MM targets. The plot displays the expected linear relationship between the inverse of melting temperature ($1/T_m$) and $R\ln(T_0-0.5P_0)$ (in which R is the gas constant, T_0 is the initial concentration of targets, and P_0 is the initial concentration of the probe) (Figure 3a). The enthalpies and entropies of the transitions from phase 1 to phase 2 ($\Delta H^0_{1\to2}$ and $\Delta S^0_{1\to2}$) were determined from these linear relationships, and the T_m value was determined by using a series of solutions containing the probe (50 nM) and various excess concentrations of 17 base targets. A three-fold difference in $\Delta H^0_{1\to2}$ and $\Delta S^0_{1\to2}$ was found for the PM target ($\Delta H^0_{1\to2}=90\pm3$ kcal mol^{-1}; $\Delta S^0_{1\to2}=240\pm17$ cal mol^{-1} K^{-1}) and the 1MM target ($\Delta H^0_{1\to2}=32\pm2$ kcal mol^{-1}; $\Delta S^0_{1\to2}=76\pm9$ cal mol^{-1} K^{-1}), which indicates that mismatched targets dissociate from the triple-stem probe more readily. On the basis of the measured enthalpy and entropy changes in the three phases, the thermodynamic stability associated with our triple-stem probe has the following hierarchy: PM target–probe hybrid $\gg$ 1MM target–probe hybrid $\approx$ probe self-hybridization. The dissociation of the probe–target duplex results in an entropy gain when the duplex dissociates and an enthalpy loss when the secondary structures reform in the probe. Because the triple-stem probe undergoes significant self-reorganization upon the dissociation (or formation) of probe–target duplexes, both the enthalpic and entropic contributions to the free energy of the probe–target dissociated state, especially in the presence of a mismatched base pair, lead to significantly improved specificity.

To further elucidate the origins of probe specificity, we constructed free-energy diagrams of the probe in equilibrium with its targets as a function of temperature ($\Delta G^0=\Delta H^0-T\Delta S^0$; Figure 3b). Phase 3 was chosen as the reference state ($\Delta G_3{}^0=0$), because under these conditions the probe and targets form random coils. The ΔG^0 values for phases 2 and 3 were calculated according to reported equations.[27] The predominant phase at each temperature is the phase with the lowest free energy. It is clear from the free-energy diagram that the transition range over which the probe–PM duplex is stable and the probe–1MM duplex is unstable is significant ($\Phi=43.6$ °C). Our triple-stem probe is therefore capable of SNP discrimination over a wide temperature range.

We have reported a reagentless, single-step, fluorescence-based method for rapid and accurate SNP detection on the basis of a target-binding-induced conformational change of a single, self-complementary DNA probe. Our probe can readily discriminate 62.5 nM perfectly matched target against as much as 4 μM single-base-mismatched target (a 64-fold excess) within 30 min at room temperature; in contrast, comprehensive studies revealed that robust single-mismatch discrimination is typically observed at 60–70 °C with conventional MBs.[36,37] Our probe design shares similarity with tripartite molecular beacons[38] and is elegantly simple: It is a single, chemically modified DNA strand. The current detection limit of our method is approximately 10 nM (500 ng μL^{-1}), which preempts direct analysis of genomic DNA: The concentration of genomic DNA obtained in standard phenol/chloroform extractions is typically approximately 30 ng μL^{-1}.[39] Thus, as in most MB approaches, PCR amplification is necessary prior to detection.

Importantly, the design of the triple-stem probe is straightforward and requires negligible optimization to enable the specific SNP detection reported herein. This feature offers an advantage for multitarget, parallel analysis over conventional MBs, which require significant optimization for each target sequence. Given that both DNA and RNA probes can form triple-stem structures,[26] and that our probe can be linked covalently to the surface of a solid-phase substrate, we believe that this approach may provide a scalable strategy for high-throughput SNP discovery and analysis with microarray technologies.

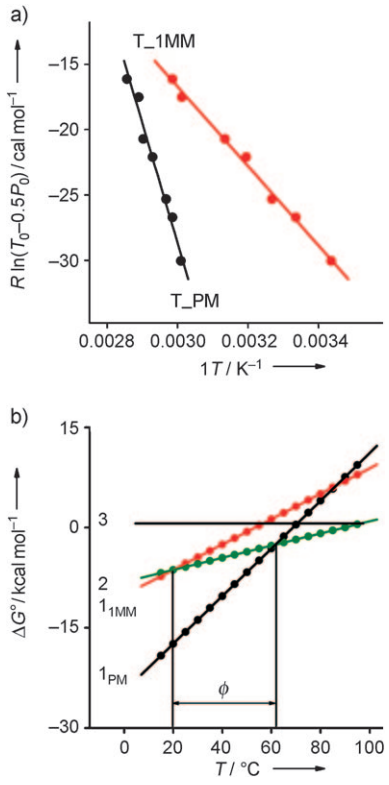

Figure 3. Determination of thermodynamic parameters. a) The thermodynamic parameters describing the dissociation of probe–target duplexes were determined for the triple-stem probe (T) with 17 base PM and 1MM targets after measuring the T_m values of the duplexes that formed at varying target concentrations. The slope of each fitted line is equal to the negative value of the enthalpy ($-\Delta H^0_{1\to2}$), and the y intercept is equal to the entropy ($\Delta S^0_{1\to2}$). b) Free-energy change for the three phases of a solution of the triple-stem probe in equilibrium with 17 base PM and 1MM targets. The difference (Φ) between the T_m values of PM duplexes (1_{PM}) and 1MM duplexes (1_{1MM}) in the triple-stem systems is 43.6 °C.

Experimental Section

Materials: All chemicals were purchased from Sigma–Aldrich, Inc. (Saint Louis, MO, USA) and used without further purification. The fluorophore/quencher-labeled DNA oligonucleotides were synthesized by Biosearch Technologies, Inc. (Novato, CA, USA), purified by C18 HPLC, and the structures confirmed by mass spectrometry (see

Figures S4 and S5 in the Supporting Information). The sequences of these modified oligomers are:

1: 5′-AGGCTGGATTTTTTATTTACCTTTTTTTAGGTAAA-(BHQ)A-CGACGGCCAGCCTTTTTTTTTTTTTCCGTCGT-T(CAL Fluor 610)-3′; **5**: 5′-AGGCTGGATTTTTTATT-TACCTTTTTTTAGGTAAA-(BHQ)A-CGGCGGCCAGCCTTTT-TTTTTTTTCCGTCGT-T(CAL Fluor 610)-3′

The perfectly matched and mismatched DNA targets were purchased from Integrated DNA Technologies Inc. (Coralville, IA, USA), and were purified by HPLC. The sequences of these DNA targets are:

15-base DNA targets: PM target: 5′-CTGGCCGTCGTTTTA-3′; 1MM target: 5′-CTGGCCGTAGTTTTA-3′

17-base DNA targets: PM target **2**: 5′-GCTGGCCGTC-GTTTTAC-3′; 1MM target **3**: 5′-GCTGGCCCTCGTTTTAC-3′; 2MM target **4**: 5′-GCTGGCCCCCGTTTTAC-3′

19-base DNA targets: PM target: 5′-GGCTGGCCGTC-GTTTTACC-3′; 1MM target: 5′-GGCTGGCCCTCGTTTTACC-3′

Fluorescence experiments: Experimental details of fluorescence denaturation experiments, kinetic experiments, the determination of melting temperatures (T_m), and the measurement of discrimination factors are provided in the Supporting Information.

Polyacrylamide gel electrophoresis: Samples with the triple-stem probe (0.5 μM) only, or the triple-stem probe (0.5 μM) hybridized with the 17 base PM (1.0 μM) or 17 base 1MM (4 μM) targets (total reaction-mixture volume: 100 μL) were equilibrated for 3 h or 3 days and then analyzed on a 10% PAGE–TBE gel (TBE = Tris (2-amino-2-hydroxymethylpropane-1,3-diol)–borate–ethylenediaminetetraacetic acid; Ready Gel, Bio-Rad Laboratories, CA, USA) at 120 V for 1 h. The gel was stained for 20 min with GelStar nucleic acid stain (Lonza, Rockland, ME, USA) and imaged with a Kodak Gel Logic EDAS 200 digital imaging system (NY, USA).

Received: January 21, 2009
Revised: March 25, 2009
Published online: May 8, 2009

Keywords: DNA · fluorescent probes · self-complementary sequences · single-nucleotide polymorphisms

[1] Y. Suh, J. Vijg, *Mutat. Res.-Fundam. Mol. Mech. Mutagen.* **2005**, *573*, 41–53.
[2] a) A. J. Schafer, J. R. Hawkins, *Nat. Biotechnol.* **1998**, *16*, 33–39; b) J. D. Luo, E. C. Chan, C. L. Shih, T. L. Chen, Y. Liang, T. L. Hwang, C. C. Chiou, *Nucleic Acids Res.* **2006**, *34*, e12.
[3] J. B. Fan, X. Q. Chen, M. K. Halushka, A. Berno, X. H. Huang, T. Ryder, R. J. Lipshutz, D. J. Lockhart, A. Chakravarti, *Genome Res.* **2000**, *10*, 853–860.
[4] K. L. Gunderson, F. J. Steemers, G. Lee, L. G. Mendoza, M. S. Chee, *Nat. Genet.* **2005**, *37*, 549–554.
[5] R. Youil, B. W. Kemper, R. G. H. Cotton, *Proc. Natl. Acad. Sci. USA* **1995**, *92*, 87–91.
[6] K. J. Livak, J. Marmaro, J. A. Todd, *Nat. Genet.* **1995**, *9*, 341–342.
[7] N. C. Nelson, P. W. Hammond, E. Matsuda, A. A. Goud, M. M. Becker, *Nucleic Acids Res.* **1996**, *24*, 4998–5003.
[8] a) U. Landegren, R. Kaiser, J. Sanders, L. Hood, *Science* **1988**, *241*, 1077–1080; b) S. Ficht, A. Mattes, O. Seitz, *J. Am. Chem. Soc.* **2004**, *126*, 9970–9981; c) S. Sando, E. T. Kool, *J. Am. Chem. Soc.* **2002**, *124*, 9686–9687.
[9] L. G. Kostrikis, S. Tyagi, M. M. Mhlanga, D. D. Ho, F. R. Kramer, *Science* **1998**, *279*, 1228–1229.
[10] L. G. Kostrikis, S. Shin, D. D. Ho, *Mol. Med.* **1998**, *4*, 443–453.
[11] T. N. Grossmann, L. Röglin, O. Seitz, *Angew. Chem.* **2007**, *119*, 5315–5318; *Angew. Chem. Int. Ed.* **2007**, *46*, 5223–5225.
[12] Y. Z. Xu, N. B. Karalkar, E. T. Kool, *Nat. Biotechnol.* **2001**, *19*, 148–152.
[13] D. M. Kolpashchikov, *J. Am. Chem. Soc.* **2005**, *127*, 12442–12443.
[14] a) O. Köhler, O. Seitz, *Chem. Commun.* **2003**, 2938–2939; b) O. Köhler, D. Venkatrao, D. V. Jarikote, O. Seitz, *ChemBioChem* **2005**, *6*, 69–77; c) E. Socher, D. V. Jarikote, A. Knoll, L. Röglin, J. Burmeister, O. Seitz, *Anal. Biochem.* **2008**, *375*, 318–330.
[15] a) A. Okamoto, K. Kanatani, I. Saito, *J. Am. Chem. Soc.* **2004**, *126*, 4820–4827; b) A. Okamoto, K. Tainaka, Y. Ochi, K. Kanatani, I. Saito, *Mol. Biosyst.* **2006**, *2*, 122–126.
[16] B. Dubertret, M. Calame, A. J. Libchaber, *Nat. Biotechnol.* **2001**, *19*, 365–370.
[17] S. Tyagi, F. R. Kramer, *Nat. Biotechnol.* **1996**, *14*, 303–308.
[18] R. Nutiu, Y. F. Li, *Nucleic Acids Res.* **2002**, *30*, 94e.
[19] G. T. Hwang, Y. J. Seo, B. H. Kim, *J. Am. Chem. Soc.* **2004**, *126*, 6528–6529.
[20] E. Socher, L. Bethge, A. Knoll, N. Jungnick, A. Herrmann, O. Seitz, *Angew. Chem.* **2008**, *120*, 9697–9701; *Angew. Chem. Int. Ed.* **2008**, *47*, 9555–9559.
[21] D. J. French, C. L. Archard, T. Brown, D. G. McDowell, *Mol. Cell. Probes* **2001**, *15*, 363–374.
[22] P. Y. Kwok, *Annu. Rev. Genomics Hum. Genet.* **2001**, *2*, 235–258.
[23] D. M. Kolpashchikov, *J. Am. Chem. Soc.* **2006**, *128*, 10625–10628.
[24] D. M. Kolpashchikov, *J. Am. Chem. Soc.* **2008**, *130*, 2934–2935.
[25] A. A. Marti, C. A. Puckett, J. Dyer, N. Stevens, S. Jockusch, J. Ju, J. K. Barton, N. J. Turro, *J. Am. Chem. Soc.* **2007**, *129*, 8680.
[26] J. Sperschneider, A. Datta, *RNA-Publ. RNA Soc.* **2008**, *14*, 630–640.
[27] G. Bonnet, S. Tyagi, A. Libchaber, F. R. Kramer, *Proc. Natl. Acad. Sci. USA* **1999**, *96*, 6171–6176.
[28] S. A. Kushon, J. P. Jordan, J. L. Seifert, H. Nielsen, P. E. Nielsen, B. A. Armitage, *J. Am. Chem. Soc.* **2001**, *123*, 10805–10813.
[29] J. Petruska, M. F. Goodman, *J. Biol. Chem.* **1995**, *270*, 746–750.
[30] H. Du, C. M. Strohsahl, J. Camera, B. L. Miller, T. D. Krauss, *J. Am. Chem. Soc.* **2005**, *127*, 7932–7940.
[31] R. Jin, G. Wu, Z. Li, C. A. Mirkin, G. C. Schatz, *J. Am. Chem. Soc.* **2003**, *125*, 1643–1654.
[32] M. L. Sauthier, R. L. Carroll, C. B. Gorman, S. Franzen, *Langmuir* **2002**, *18*, 1825–1830.
[33] F. Aboul-ela, D. Koh, I. Tinoco, Jr, F. H. Martin, *Nucleic Acids Res.* **1985**, *13*, 4811–4824.
[34] S. Ikuta, K. Takagi, B. R. Wallace, K. Itakura, *Nucleic Acids Res.* **1987**, *15*, 797–811.
[35] L. A. Marky, K. J. Breslauer, *Biopolymers* **1987**, *26*, 1601–1620.
[36] a) A. Tsourkas, M. A. Behlke, S. D. Rose, G. Bao, *Nucleic Acids Res.* **2003**, *31*, 1319–1330; b) A. Ramachandran, J. Flinchbaugh, P. Ayoubi, G. A. Olah, J. R. Malayer, *Biosens. Bioelectron.* **2004**, *19*, 727–736.
[37] F. J. Steemers, J. A. Ferguson, D. R. Walt, *Nat. Biotechnol.* **2000**, *18*, 91–94.
[38] A. Tsourkas, M. A. Behlke, G. Bao, *Nucleic Acids Res.* **2002**, *30*, 4208–4215.
[39] K. E. Pilcher, P. Fey, P. Gaudet, A. S. Kowal, R. L. Chisholm, *Nat. Protoc.* **2007**, *2*, 1325–1328.